

Seasonality of reactive nitrogen oxides (NO_y) at Neumayer Station, Antarctica

R. Weller,¹ A. E. Jones,² A. Wille,³ H.-W. Jacobi,¹ H. P. McIntyre,⁴ W. T. Sturges,⁴ M. Huke,⁵ and D. Wagenbach⁵

Received 30 April 2002; revised 9 July 2002; accepted 15 August 2002; published 3 December 2002.

[1] NO, NO_y (total reactive nitrogen oxides), gaseous HNO₃, and particulate nitrate (p-NO₃⁻) were measured at Neumayer Station from February 1999 to January 2000. In addition, during February 1999, the NO_y component species peroxyacetyl nitrate (PAN) and methyl, ethyl, i-propyl, and n-propyl nitrates were determined. We found a mean NO_y mixing ratio of 46 ± 29 pptv, with significantly higher values between February and end of May (58 ± 35 pptv). Between February and November, the (HNO₃ + p-NO₃⁻)/NO_y ratio was extremely low (around 0.22) and in contrast to NO_y the seasonality of p-NO₃⁻ and HNO₃ showed a distinct maximum in November and December, leading to a (HNO₃ + p-NO₃⁻)/NO_y ratio of 0.66. Trajectory analyses and radioisotope measurements (⁷Be, ¹⁰Be, ²¹⁰Pb, and ²²²Rn) indicated that the upper troposphere or stratosphere was the main source region of the observed NO_y with a negligible contribution of ground-level sources at northward continents. Frequent maxima of NO_y mixing ratios up to 100 pptv are generally associated with air mass transport from the free troposphere of continental Antarctica, while air masses with the lowest NO_y mixing ratios were typically advected from the marine boundary layer. *INDEX TERMS*: 0330

Atmospheric Composition and Structure: Geochemical cycles; 0322 Atmospheric Composition and Structure: Constituent sources and sinks; 0365 Atmospheric Composition and Structure: Troposphere—composition and chemistry; 0368 Atmospheric Composition and Structure: Troposphere—constituent transport and chemistry; *KEYWORDS*: reactive nitrogen oxides, nitric acid, NO, alkyl nitrates

Citation: Weller, R., A. E. Jones, A. Wille, H.-W. Jacobi, H. P. McIntyre, W. T. Sturges, M. Huke, and D. Wagenbach, Seasonality of reactive nitrogen oxides (NO_y) at Neumayer Station, Antarctica, *J. Geophys. Res.*, 107(D23), 4673, doi:10.1029/2002JD002495, 2002.

1. Introduction

[2] Reactive nitrogen oxides generally refer to the sum of oxidized nitrogen species in the atmosphere (NO_y = NO + NO₂ + HNO₃ + HNO₂ + HONO + PAN + organic nitrates + NO₃ + 2 N₂O₅ + XONO₂... where PAN is peroxyacetyl nitrate, and X is a halogen atom). Atmospheric chemistry of NO_y components is closely linked with interconversion between its members, while the percentage that each individual component contributes to the total NO_y budget clearly varies at different locations and with time in the atmosphere [e.g., Thakur *et al.*, 1999]. Due to the role of NO and NO₂ in determining the oxidation capacity of the troposphere, knowledge of the natural background concentration of oxidized nitrogen compounds is pivotal in judging

the impact of human activity on the oxidizing capacity of the Earth's atmosphere [e.g., Logan, 1983; Kleinman, 1994]. Apart from the remote South Pacific and South Atlantic, Antarctica seems to be the only remaining area where the almost natural tropospheric NO_y budget may be studied. Interestingly, recent field campaigns at Neumayer Station have revealed photochemical NO_x production from the upper firm layer [Jones *et al.*, 2000], a process which may have a dramatic impact on the summertime NO_x budget and boundary layer photochemistry in central Antarctica [Davis *et al.*, 2001]. Another motivation to investigate the chemistry and budget of NO_y especially at high latitudes arises in view of serious deficits in the interpretation of nitrate signals in ice cores. Ice cores carry an invaluable potential in providing proxies to elucidate climate and chemical composition of the past atmosphere, and hence to assess the evolution of our present one. While nitrate is one of the most abundant ionic impurities of polar ices, translation into past atmospheric changes remained enigmatic [Wolff, 1995; Wagenbach, 1996] since even the major source of background NO_y (and hence nitrate in the ice) is not well known. Both lightning and downward transport of N₂O derived NO_y from the stratosphere were suggested as the origin of nitrate in Antarctica [Legrand and Delmas, 1986; Wagenbach *et al.*, 1998], whereas no anthropogenic effect could be revealed [Legrand and Mayewski,

¹Alfred-Wegener-Institut für Polar- und Meeresforschung, Bremerhaven, Germany.

²British Antarctic Survey, Natural Environment Research Council, High Cross, Cambridge, UK.

³Metrohm AG, Herisau, Switzerland.

⁴School of Environmental Sciences, University of East Anglia, Norwich, UK.

⁵Institut für Umweltphysik, Universität Heidelberg, Heidelberg, Germany.

1997]. In contrast to Antarctica, Arctic ice core nitrate records [Legrand and Mayewski, 1997; Fischer et al., 1998] and atmospheric measurements [Honrath and Jaffe, 1992; Wofsy et al., 1992] clearly revealed a dramatic impact of anthropogenic emissions on the Arctic NO_y budget.

[3] In this paper we present reactive nitrogen oxide measurements conducted during the PEAN'99 summer campaign (Photochemical Experiment at Neumayer, February 1999) and the succeeding overwintering period at the German Antarctic research station Neumayer. During February 1999, mixing ratios of NO_y and the individual components NO , NO_2 , HNO_3 , particulate nitrate (p-NO_3^-), PAN, and methyl, ethyl, *i*-propyl, and *n*-propyl nitrates (CH_3ONO_2 , $\text{C}_2\text{H}_5\text{ONO}_2$, $\text{C}_3\text{H}_7\text{ONO}_2$, and $(\text{CH}_3)_2\text{CHONO}_2$, respectively) were determined, while during the overwintering period from March 1999 to January 2000 the measuring program was restricted to NO , NO_y , HNO_3 , and p-NO_3^- . For the first time, year-round NO_y and NO measurements in Antarctica could be realized allowing the observed NO_y and nitrate seasonality to be discussed in terms of source assignment and associated implications for the interpretation of Antarctic nitrate ice core records under present-day climatic conditions. These evaluations are backed up by year-round observations of atmospheric radioisotope concentrations (^7Be , ^{10}Be , and ^{210}Pb). In addition, supporting information on air mass characterization arriving at Neumayer came from daily back trajectory studies.

2. Measurement Techniques

2.1. Measurement Site and Meteorological Conditions

[4] All measurements were made either at, or close to, the Air Chemistry Observatory, Neumayer Station ($70^\circ 39'\text{S}$, $8^\circ 15'\text{W}$), where meteorological data are collected continuously [König-Langlo et al., 1998]. During the summer months, the bay and the nearby ice edge are mainly free of sea ice and there is always open water present. Other than a few nunataks about 100 km south of the station there are no ice-free land surfaces near Neumayer, and the probability of contact with air masses from ice-free continents is small. The prevailing winds are from the east, but with strong switches to westerly winds from time to time. The air mass transport pattern to Neumayer Station was investigated by Kottmeier and Fay [1998] and a more detailed picture on the climatology at Neumayer Station is given by König-Langlo et al. [1998].

[5] Local pollution by vehicles and the base itself is a potential problem for many measurements concerning the background status of the Antarctic troposphere. Consequently, a central aspect of the technical concept of the air chemistry observatory lies in the possibility of contamination-free sampling of aerosols and trace gases. This is realized by several means: the Air Chemistry Observatory is situated in a clean air facility approximately 1.5 km south of Neumayer. Due to the fact that northerly wind directions are very rare, contamination from the base can be excluded for most of the time. The power supply (20 kW) is provided by cable from the main station, thus no fuel driven generator is operated in the observatory vicinity. Contamination-free sampling is controlled by the permanently recorded wind velocity, wind direction and by the condensation nuclei (CN) concentration. Contamination was indicated if one of

the following criteria was given: wind direction within a $330^\circ\text{--}30^\circ$ sector, wind velocity $<2.2\text{ m s}^{-1}$ and/or CN concentrations (measured by a TSI CNC3022A particle counter) $>1200\text{ cm}^{-3}$ during summer, $>800\text{ cm}^{-3}$ during spring/autumn and $>400\text{ cm}^{-3}$ during winter. The CN threshold values were chosen on the basis of our nearly 20-year long CN record from Neumayer, demonstrating that CN concentrations above the corresponding levels can usually be traced back to local pollution.

[6] For the present study, daily 5-day back trajectories were calculated by the German Weather Service (Deutscher Wetterdienst, DWD) based on the global model of the DWD. In all cases the air masses reached Neumayer at 1200 UTC. Throughout this work the time is given in UTC, corresponding to a shift of +32 min relative to the solar time and trace compound concentrations are given in pptv, ppbv, or at scm^{-3} (parts per 10^{12} or 10^9 by volume or atoms per standard m^3).

2.2. NO , NO_2 , and NO_y

[7] We measured NO , NO_2 , and NO_y using two chemiluminescence detectors coupled with a photolytical NO_2 and an Au/CO catalyzed NO_y convertor, respectively. NO_y was determined by reduction to NO (gold catalyst at 300°C with 0.3% CO) and a chemiluminescence detector (Eco Physics CLD 780 TR). The values for NO_y are derived from 200-s integrations, binned to give 30-min averages. The instruments were run under controlled conditions, including checks and tests for instrument performance carried out on a daily basis throughout the year as well as prior to leaving for Antarctica. While a detailed discussion of accuracy determination and measurement technique is given by Jones et al. [1999, 2001] and Weller and Schrems [1996], only some details, concerning the reliability of the NO_y time series, will be reported here. The conversion efficiency of the NO_y convertor was checked weekly with NO_2 using NIST traceable NO standard mixtures (1.03 ± 0.05 ppmv NO in N_2 , Messer Griesheim, Germany) for dynamic dilution to the range between 3 and 10 ppbv NO. Former tests revealed that the instrument showed a linear response down to at least 25 pptv NO [Weller and Schrems, 1996]. NO_2 was generated by gas phase titration of NO calibration mixtures with ozone. The conversion efficiency factor was found to be essentially constant at 0.95 ± 0.03 , showing no systematic change over 1 year of continuous operation of the convertor. Similarly, laboratory experiments were carried out to determine the conversion efficiency of HNO_3 both before leaving for Antarctica and on return. The HNO_3 conversion efficiency was found to vary between 0.72 and 0.93. We forwent cleaning of the gold catalyst since it seemed to enhance the conversion efficiency only for a few hours. In addition, the response of the NO detector was determined before, during, and after the overwintering with different certified NO calibration mixtures, showing that the sensitivity of the NO detector remained essentially stable. At the end of the measuring period in January 2000, NO_y mixing ratios were comparable with those measured in January/February 1997 [Weller et al., 1999] and February 1999, which underlines the stable performance of the equipment.

[8] Considerable care must be taken when evaluating NO_y data, as the operationally defined number NO_y^* resulting from the measurement may not represent the real, above

Table 1. Mixing Ratios and Error Limits (\pm Accuracy) of Individual NO_y Component Species Measured During PEAN'99 Campaign

Date	CH_3ONO_2 [pptv]	$\text{C}_2\text{H}_5\text{ONO}_2$ [pptv]	$(\text{CH}_3)_2\text{CHONO}_2$ [pptv]	$\text{C}_3\text{H}_7\text{ONO}_2$ [pptv]	PAN [pptv]	HNO_3 [pptv]	$\text{NO} + \text{NO}_2$ [pptv]	Sum [pptv]	NO_y^* [pptv]
8 February	8.0 ± 0.6	1.8 ± 0.13	1.2 ± 0.1	0.7 ± 0.06	8.7 ± 3.0	2.6 ± 0.6	7.6 ± 4.0	30.6 ± 5.1	35.1 ± 12
17 February	8.5 ± 0.65	1.9 ± 0.13	0.9 ± 0.1	—	9.0 ± 3.0	3.6 ± 0.8	4.6 ± 3.5	28.6 ± 4.8	45.1 ± 16
18 February	9.4 ± 0.7	2.2 ± 0.15	0.7 ± 0.07	0.9 ± 0.07	9.1 ± 3.0	3.6 ± 0.8	2.1 ± 2.0	28.1 ± 4.0	42.2 ± 15
19 February	10.8 ± 0.8	2.9 ± 0.2	1.3 ± 0.12	1.0 ± 0.08	11.3 ± 3.0	2.3 ± 0.5	3.4 ± 3.0	33.1 ± 4.4	24.7 ± 8.6
20 February	10.7 ± 0.8	2.9 ± 0.2	1.1 ± 0.12	1.1 ± 0.09	12.5 ± 3.0	2.3 ± 0.5	1.6 ± 1.6	32.2 ± 3.6	16.0 ± 5.6

NO , NO_2 , and NO_y^* represent mean values over the respective HNO_3 sampling interval, while the alkyl nitrate data correspond to sampling periods of typically 30 min.

defined NO_y in the ambient atmosphere, for our data NO_y^* includes the sum of inorganic oxidized nitrogen and PAN plus the converted fraction of the light alkyl nitrates. As discussed by Jones *et al.* [1999], we do not consider that it will include p-NO_3^- . Recognizing the difficulties with HNO_3 sampling because of uptake to surfaces, some proportion of HNO_3 is likely to be missing from the measured NO_y^* . We determined the inlet efficiency factor to be 0.7 ± 0.2 . This causes no substantial problems, however, as HNO_3 mixing ratios were in the lower pptv range, except of the period from November to January, when the NO_y^* values were corrected for inlet efficiency (0.7) and conversion efficiency (0.8). Much more problematic is the conversion efficiency of methyl nitrate, which seems to be a dominant NO_y^* component species at Neumayer at least during summer [Jones *et al.*, 1999]. To our knowledge, conversion efficiencies for methyl nitrate are not available and we did not succeed in developing a suitable calibration source for the NO_y convertor. During the PEAN'99 campaign, coinciding alkyl nitrates, HNO_3 , PAN, NO_x , and NO_y^* measurements were available for an overall period of 72 hours. Assuming a uniform conversion efficiency of 1.0 for all components, a comparison of the budget from the sum of the individual compounds and the measured NO_y^* showed that NO_y^* agrees on average within the error limits (Table 1). This is consistent with results obtained with the same convertor type at Jungfraujoch, Switzerland by Zellweger *et al.* [2000]. Here NO_y^* was 22% higher than the individually measured NO_y components. Zellweger *et al.* [2000] attribute this discrepancy to the presence of alkyl nitrates, which were not measured.

[9] In order to ensure that the influence of local NO_y sources or instrumental artifacts did not affect the data presented here, the raw NO_y^* and NO data records were subject to a detailed and conservative screening procedure. Exclusively the diesel generator of the nearby Neumayer Station and frequent motor vehicle usage during polar summer must be considered as possible contamination source. Contamination was indicated by the criteria described in section 2.1. In addition, the NO_y^* convertor showed disturbingly high background noise after calibration procedures or instrument failures caused by occasional power outages. All NO_y^* data recorded within such periods were discarded and not considered for further evaluation. In all, we obtained reliable NO_y^* data from about 73.1% of the total available time between 1 February 1999 and 17 January 2000. The most extensive data losses of about 77% occurred in February when instrumental problems in the setup phase and detailed performance tests were conducted.

[10] The precision of the NO_y^* measurement on a 2σ basis was determined to be around $\pm 20\%$ in the concen-

tration range between 10 and 100 pptv. The accuracy is highly dependent on the composition of ambient NO_y , given the possible differences in conversion efficiency of the various components. Assuming that the conversion efficiencies of all component species not experimentally determined here was 0.75 ± 0.25 , the overall accuracy of the NO_y^* measurement was $\pm 35\%$ from February to November. From early November to late January, the portion of HNO_3 was between 21% and 41% of the total NO_y^* amount. Therefore the variable transmission and conversion efficiencies of HNO_3 were most decisive leading to an accuracy of $\pm 31\%$ during this period.

2.3. HNO_3 and p-NO_3^-

[11] During the PEAN'99 summer campaign nitric acid and p-NO_3^- were sampled for 24-hour time periods using a 3-stage PFA filter holder system, including a Teflon and two nylon (Nylasorb) filters (all $1\ \mu\text{m}$ pore size). During the overwintering a Teflon/nylon/cellulose filter combination (Whatman 541 cellulose filter impregnated with K_2CO_3 to sample acidic gases and SO_2) was used and the temporal resolution was 7 days. The filter systems were housed within the Neumayer Air Chemistry Observatory. Ambient air was drawn through a ventilated stainless steel inlet stack (total height 8–9 m above the snow surface). While the Teflon filter collected p-NO_3^- , gaseous HNO_3 passing the Teflon filter or reemitted from it was collected by the nylon backup filters. For the 24-hour (7 days) sampling period, derived errors were 21% (15%) and 9% (7%) for HNO_3 and p-NO_3^- , respectively, with a combined error for total inorganic nitrate ($\text{HNO}_3 + \text{p-NO}_3^-$) of 11% (9%). The detection limit, derived from 2σ of the blank values, was found to be 1 pptv (about 0.5 pptv) for both p-NO_3^- and gaseous nitrate. Further details are described by Jones *et al.* [1999].

2.4. Additional Measurements During PEAN'99: PAN and Alkyl Nitrates

[12] Preconditioned 800 and 3200 mL stainless steel flasks were filled to roughly 3.2 bar at regular intervals during the campaign, using a metal bellows pump after thorough flushing of the whole system with ambient air. Whenever possible, flasks were filled at ground level roughly 50 m upwind of the Air Chemistry Observatory. The whole air samples were analyzed using a gas chromatograph equipped with an electron capture detector (ECD, Ni-63 foil). The respective accuracies were $\pm 7.5\%$ for CH_3ONO_2 , $\pm 7\%$ for $\text{C}_2\text{H}_5\text{ONO}_2$, $\pm 9.2\%$ for $\text{C}_3\text{H}_7\text{ONO}_2$, and $\pm 8\%$ for $(\text{CH}_3)_2\text{CHONO}_2$. In total we analyzed 96 flasks for alkyl nitrates, sampled between 7 and 23 February. The mean mixing ratios (\pm s.d.) were 9.5 ± 1.4 pptv CH_3ONO_2 , 2.3 ± 0.5 pptv $\text{C}_2\text{H}_5\text{ONO}_2$, 1.1 ± 0.8

$C_3H_7ONO_2$, and 1.2 ± 0.5 pptv $(CH_3)_2CHONO_2$. In the course of this study we found that the calibration used to calculate $RONO_2$ mixing ratios in our previous paper on NO_y^* speciation at Neumayer in 1997 [Jones *et al.*, 1999] may have been in error. The calibration of methyl and ethyl nitrates presents particular challenges, requiring synthesis of the pure compounds, and coanalysis of dynamically diluted effusion from diffusion tubes by both chemiluminescence and ECD. Of particular note was the discovery that humidity levels have a profound effect on the sensitivity and reproducibility of the ECD determination of $RONO_2$. A new calibration was performed with a humidification system in place and the 1997 results were reassessed in the light of this [McIntyre, 2001]. $RONO_2$ mixing ratios are now thought to have been overestimated by about a factor of 3, explaining why NO_y^* estimated from summation of individual species did, on occasions, exceeded the direct chemiluminescence measurement of NO_y^* . Applying the revised calibration to the 1997 data resulted in an estimated average NO_y^* from summation of species of 25 ± 5 pptv, lower than the original estimate of 39 ± 6 pptv, and within the error of the mean chemiluminescence measurement of 30 ± 20 pptv. Only methyl and ethyl nitrates were considered in the 1997 study, but the work here shows that C_3 nitrates contribute at most only one or two pptv of NO_y^* , and there was no evidence of significant levels of higher alkyl nitrates in the ECD traces either then or in the current study. The revised measurements of methyl and ethyl nitrate from 1997 (10 ± 2 and 3 ± 1 pptv, respectively) are now in good agreement with the averages from this study (see above).

[13] The method for the PAN measurements is based on electron capture gas chromatography with cryogenic pre-concentration technique [Schrimpf *et al.*, 1995]. Details of the commercial analyzer (Meteorologie Consult GmbH, Glashütten, Germany) were recently described [Jacobi *et al.*, 1999]. A PAN detection limit of 5 pptv was obtained referring to two times the standard deviation of the noise. Multipoint calibrations were performed at the beginning and at the end of the campaign and showed good agreement, resulting in an estimated overall accuracy of $\pm 15\%$ or ± 3 pptv, whatever is higher [Jacobi *et al.*, 2000].

2.5. 7Be , ^{10}Be , ^{210}Pb , and Solar Irradiance Measurements

[14] These measurements are part of the long-term measuring program carried out since 1983 at Neumayer (<http://www.awi-bremerhaven.de/GPH/SPUSO.html>). Aerosol borne 7Be , ^{10}Be , and ^{210}Pb were collected on cellulose filters ($2 \times$ Whatman 541 in series, diameter 240 mm) by continuous high volume aerosol sampling ($120 \text{ m}^3 \text{ hr}^{-1}$, sampling interval 2 weeks) through the stainless steel stack of the Air Chemistry Observatory. After return to the Heidelberg laboratory the 7Be and ^{210}Pb activities were determined by high resolution γ -spectroscopy as described by Wagenbach *et al.* [1988], ^{10}Be was measured by accelerator mass spectroscopy. 1σ counting errors were generally between 5% and 15% for 7Be (depending on the decay time before analyses) and typically 10% for ^{210}Pb . UV solar radiation was measured routinely by an UV radiometer (Eppley, USA, 300–370 nm) and an UV-B spectroradiometer covering the spectral range from 280 to 320 nm with a spectral resolution better than 1.35 nm at an absolute

wavelength precision of 0.01 nm and a detection threshold of $10^{-7} \text{ W m}^{-2} \text{ nm}^{-1}$ [Seckmeyer *et al.*, 1998].

3. Results and Discussion

3.1. NO_y^* Data Presentation

[15] In Figure 1 the entire NO_y^* time series is presented. Note that due to high HNO_3 mixing ratios, NO_y^* data between 1 November 1999 (day of the year, DOY = 305) and 17 January 2000 (DOY = 382) was corrected for the inlet and conversion efficiency of HNO_3 . In Figure 2, HNO_3 , the sum of $p\text{-NO}_3^-$ and HNO_3 (total nitrate) and the mean NO_y^* mixing ratio averaged over each aerosol sampling interval are shown. A similar seasonal cycle of HNO_3 and total nitrate mixing ratios was measured through the years 1997, 1998, and 2000. From the NO_y^* time series the following overall picture emerges: NO_y^* mixing ratios showed a broad maximum during late summer and fall, while a minimum could be observed during polar night. The frequency distribution of the NO_y^* mixing ratios matches a normal distribution skewed to higher values (Table 2). A comparison of the $p\text{-NO}_3^-/HNO_3$ with NO_y^* data revealed that except for the months November, December, and January the HNO_3/NO_y^* and the $(HNO_3 + p\text{-NO}_3^-)/NO_y^*$ ratios were rather low. Only from November to January, HNO_3 seemed to be a major NO_y^* component species (Table 3).

[16] As mentioned in the experimental section, measuring reactive nitrogen oxides by catalytic reduction/chemical luminescence technique (CR/CL) may be susceptible to several artifacts. Although a discrepancy between the NO_y^* determined by CR/CL and the sum of individual NO_y component species was not confirmed by our limited data set, we will assess if the presented features of the NO_y^* time series might be caused by systematic composition change of NO_y , though the sum of NO_y compounds was apparently constant. If we assume an uniform and high conversion efficiency of the reactive and thermally unstable component species PAN, NO_3 , HNO_4 , N_2O_5 , $ClONO_2$, and $BrONO_2$, which may constitute a significant part of the NO_y budget during polar night, the most critical NO_y component is CH_3ONO_2 due to its probably low conversion efficiency. But even assuming a conversion efficiency as low as 0.5, methyl nitrate variations with amplitudes higher than 20 pptv would have been needed to explain the NO_y^* maxima observed from March to June. This is rather unrealistic, especially considering the relatively constant methyl nitrate mixing ratios around 9 pptv observed in February. Up to now the source of methyl nitrate is unclear, although recent studies point to a marine origin [Talbot *et al.*, 2000]. However, during the PEAN'99 campaign trajectories did not indicate that advection of marine air was linked with enhanced methyl nitrate mixing ratios. It is likely that marine emissions are widespread throughout the Southern Hemisphere. Combined with its relatively long tropospheric residence time, especially in higher latitudes, a reasonably uniform background concentration of methyl nitrate could be anticipated throughout the year. Flocke *et al.* [1998] discussed gas phase production of CH_3ONO_2 that could be relevant for the upper troposphere and lower stratosphere. Regarding the very low CH_3ONO_2/NO_y ratio of <0.1 found in upper tropospheric air [Talbot *et al.*, 2000],

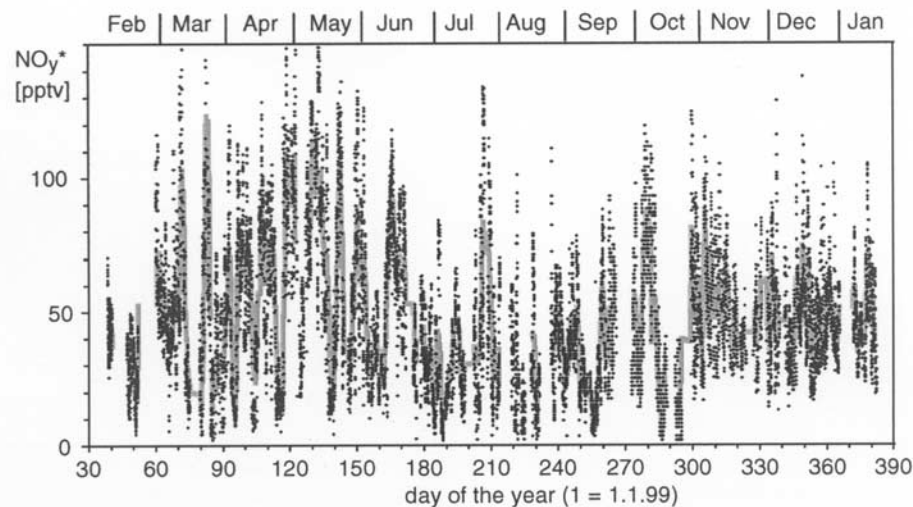


Figure 1. Measured NO_y^* time series. Dots represent 30-min averages, and the gray line corresponds to 24-hour running means.

an impact of varying methyl nitrate mixing ratios on the observed NO_y^* seasonality may be negligible.

3.2. Photochemical Aspects

[17] Reemission of deposited NO_y [Weller et al., 1999] and solar radiation induced NO_x emissions from the firm

layer [Honrath et al., 1999; Jones et al., 2000, 2001] may partly be responsible for diurnal NO_y^* variations associated with NO_y^* maxima in the late afternoon frequently observed from November 1999 to January 2000 (Figure 3). Similar to our results obtained in January and February 1997 [Weller et al., 1999], the occurrence of such diurnal NO_y^* cycles during

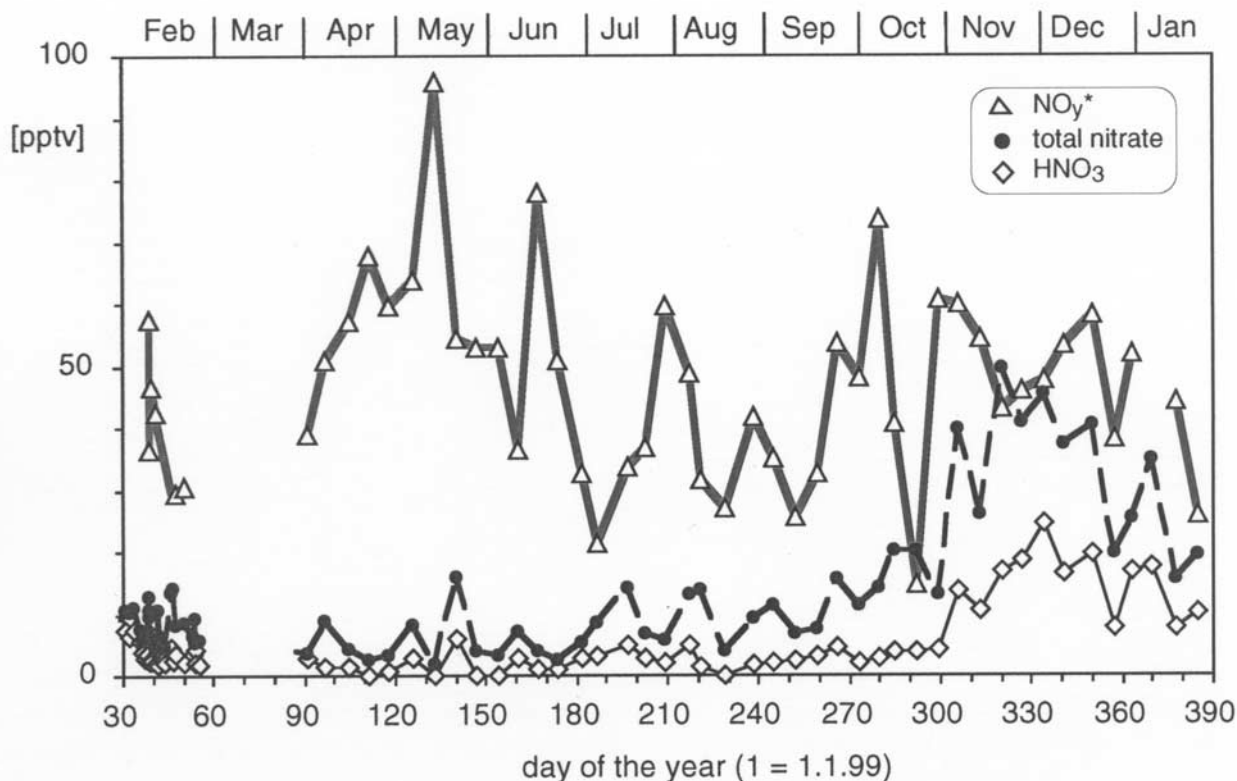


Figure 2. Seasonality of NO_y^* (triangles) in comparison with HNO_3 (diamonds) and total nitrate (closed circles). The NO_y^* mixing ratios equal averages for corresponding aerosol sampling periods (1 week).

Table 2. Statistics of the NO_y^* Measurement at Neumayer

Period	NO_y^* mean \pm s.d. [pptv]	Skewness
1 February to 31 May (DOY 32–151)	58 \pm 35	0.99
1 June to 17 January (DOY 152–382)	44 \pm 23	0.63
All data (DOY 32–382)	49 \pm 29	1.05

polar summer was linked with the variability of the surface inversion strength and the actinic radiation. Apart from these special cases, NO_y^* signals and surface inversion strength (defined as the temperature difference between 10 and 2 m altitude, ΔT_{10m-2m}) or radiation were generally not correlated, indicating that this process appeared to be secondary regarding the NO_y^* balance at Neumayer. However, recent investigations indicate that in continental Antarctica photochemically recycled nitrate from the upper firn layer, i.e., emissions of NO_x ($=\text{NO} + \text{NO}_2$) produced by postdepositional photolysis of nitrate, leads to a dramatic accumulation of NO within the flat surface inversion layer [Davis *et al.*, 2001]. There, and in coastal sites with pronounced katabatic winds, during austral summer a significant if not dominant part of the NO_y^* balance might be controlled by this process. Although Neumayer is clearly not among such sites, the seasonal maximum of the NO signals appears at the end of the ozone hole period in early December. In Figure 4, NO mixing ratios are presented in comparison with short wave UV radiation (measured at 300 nm, spectral width 1.35 nm), which may have caused an increased nitrate photolysis within the upper firn layer during this period. Note, that the observed NO maximum during early December was primarily not caused by enhanced NO_2 photolysis rates. NO_2 photolysis frequencies are roughly comparable to the UV irradiance between 300 and 370 nm as measured by the Eppley radiometer [Junkermann *et al.*, 1989] exhibiting a nearly constant level from early December to the end of January (Figure 4). However, a statistically significant correlation between shortwave UV-radiation and near surface NO mixing ratios was not found, most probably blurred by the variable stability of the boundary layer. In addition, our NO levels were an order of magnitude lower than the values found by Davis *et al.* [2001] at South Pole with NO_y^* mixing ratios showing no significant increase. On the other hand, it is well known that especially in central Antarctica a large part of deposited nitrate is exposed to postdepositional losses [e.g., Röthlisberger *et al.*, 2002]. One may speculate whether the maximum in HNO_3 and p- NO_3^- mixing ratios can partly be attributed to enhanced HNO_3 and NO_x emissions from central Antarctic snowfields, but an assessment of this problem would deserve dedicated model calculations.

3.3. Major NO_y^* Source Assignment

[18] From March to May a peculiar alternation between high and low NO_y^* mixing ratios was observed. This period,

which also embraces the seasonal NO_y^* maximum, coincides with the beginning of the polar winter and the development of the polar vortex [Schoeberl and Hartmann, 1991]. Regarding 5-day back trajectories it emerged that in most cases a change occurred from advection of marine boundary layer air masses resulting in low NO_y^* mixing ratios to down mixing of air parcels from continental Antarctica causing events of increasing or maximum NO_y^* signals (Figure 5). Note that only trajectories of the following two categories are presented: (1) air masses from the marine boundary layer below the 800 hPa level and (2) air masses from the free troposphere over continental Antarctica, originating above the 700 hPa level. The first category showed mean NO_y^* mixing ratios of 44 ± 18 pptv, while the latter bore significantly higher NO_y^* levels of 63 ± 26 pptv. The remaining trajectories were less characteristic, i.e., a clear classification in marine boundary layer or continental free troposphere air masses was not possible. Although no trajectory could eventually be traced back to the stratosphere and in some cases a clear connection between air mass origin and NO_y^* extrema was not evident, it is obvious that during this period low NO_y^* mixing ratios were preferentially found in marine boundary layer air while higher NO_y^* levels could be assigned to advection from the free troposphere above the inland ice. Regarding the whole NO_y^* record, this differentiation was not so pronounced and barely significant: advection from marine areas within 800–1000 hPa showed NO_y^* mixing ratios of 40 ± 15 pptv, while NO_y^* mixing ratios in air masses from the free troposphere of continental Antarctica (above 700 hPa) were only slightly higher (49 ± 24 pptv, Figure 6).

[19] ^7Be , whose equilibrium mixing ratios steadily increase with altitude showing a maximum in the lower stratosphere, is only a poor tracer for stratospheric intrusions. Actually, the observed NO_y^* record clearly showed no correlation with ^7Be activity levels at Neumayer. As outlined by Wagenbach *et al.* [1988], ^7Be activities have to be normalized by ^{210}Pb activities in order to cancel the down-mixing efficiency from the free troposphere to the surface layer. By this means, $^7\text{Be}/^{210}\text{Pb}$ ratios are a suitable tracer for down-mixing of stratospheric or upper tropospheric air masses. Figure 7 presents the mean NO_y^* mixing ratios during corresponding radioisotope sampling intervals (2 weeks) and the calculated $^7\text{Be}/^{210}\text{Pb}$ activity ratio. Although the $^7\text{Be}/^{210}\text{Pb}$ maximum preceded the NO_y^* maximum, the overall seasonality looks quite similar and a significant positive covariance exists (90% significance level, $N = 25$, $r = 0.35$). In contrast, ^{210}Pb activity was anticorrelated (99.5% significance level, $N = 25$, $r = 0.56$). Again atmospheric ^{222}Rn whose major sources are the ice-free continents is measured routinely at Neumayer and exhibits there regular enhanced levels on the diurnal timescale (so-called radon storms) showed virtually no

Table 3. $\text{HNO}_3/\text{NO}_y^*$ and $(\text{HNO}_3 + \text{p-NO}_3^-)/\text{NO}_y^*$ Ratios Measured at Neumayer

Period	$\text{HNO}_3/\text{NO}_y^*$ (\pm s.d.)	$(\text{HNO}_3 + \text{p-NO}_3^-)/\text{NO}_y^*$ (\pm s.d.)
1 February to 31 October (DOY 32–304)	0.06 \pm 0.05	0.22 \pm 0.2
1 November to 31 January (DOY 305–382)	0.31 \pm 0.1	0.69 \pm 0.23
All data (DOY 32–382)	0.12 \pm 0.1	0.33 \pm 0.3

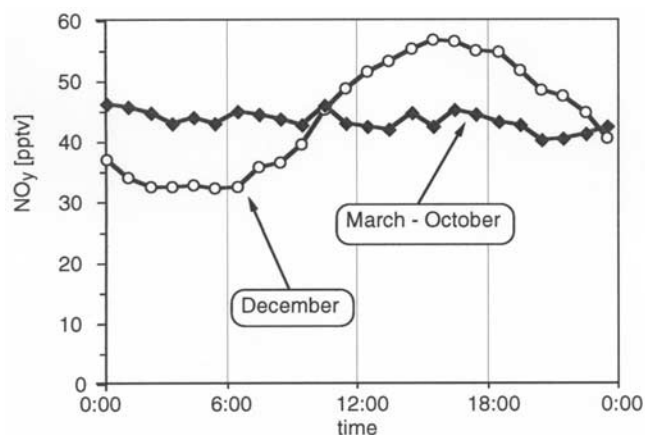


Figure 3. Mean diurnal cycles of NO_y^* (filled diamonds from March to October; circles for December). Each time interval represents the corresponding average over the mentioned observation period. The daily maximum of the solar UV radiation is at 1232 UTC (local noon).

correlation with NO_y^* mixing ratios. In addition, black carbon (BC), which can be regarded as a tracer for biomass burning, clearly showed a different seasonality compared with NO_y^* in Antarctica. BC concentrations

measured since 1995 at Neumayer with an aethalometer (Magee Scientific AE10iE) are maximal between July and October, while at Halley [Wolff and Cachier, 1998] and South Pole [Bodhaine, 1995] the seasonal BC maxima appear in October. All these findings argue against a NO_y ground-level source at northward continents favoring instead a stratospheric or upper tropospheric NO_y origin.

[20] In the following we try to assess the NO_y associated with stratospheric air by using ^{10}Be and ^7Be data from Neumayer. Unfortunately, the ^{10}Be data for 1999 are only seasonally resolved (i.e., 3-month means), but for the years 1983–1986 ^{10}Be records with 2 weeks and 1990/1991 with monthly resolution were available. Therefore we used a normalized ^{10}Be mean annual cycle based on the high resolution data set and scaled to the mean of the 1999 data. Another critical point is the assumption of equal tropospheric lifetimes of the Be-bearing aerosol (about 30 days according to Shaw [1982]) and NO_y (Logan *et al.* [1981] estimated a free tropospheric HNO_3 residence time of 5–55 days for 4–10 km altitude). Our calculations are based on a simple two-box approach under steady state assumptions as previously described by Raisbeck *et al.* [1981], which allows elucidation of the contribution of stratospheric air arriving at ground level from ^{10}Be and ^7Be measurements. The stratospheric and

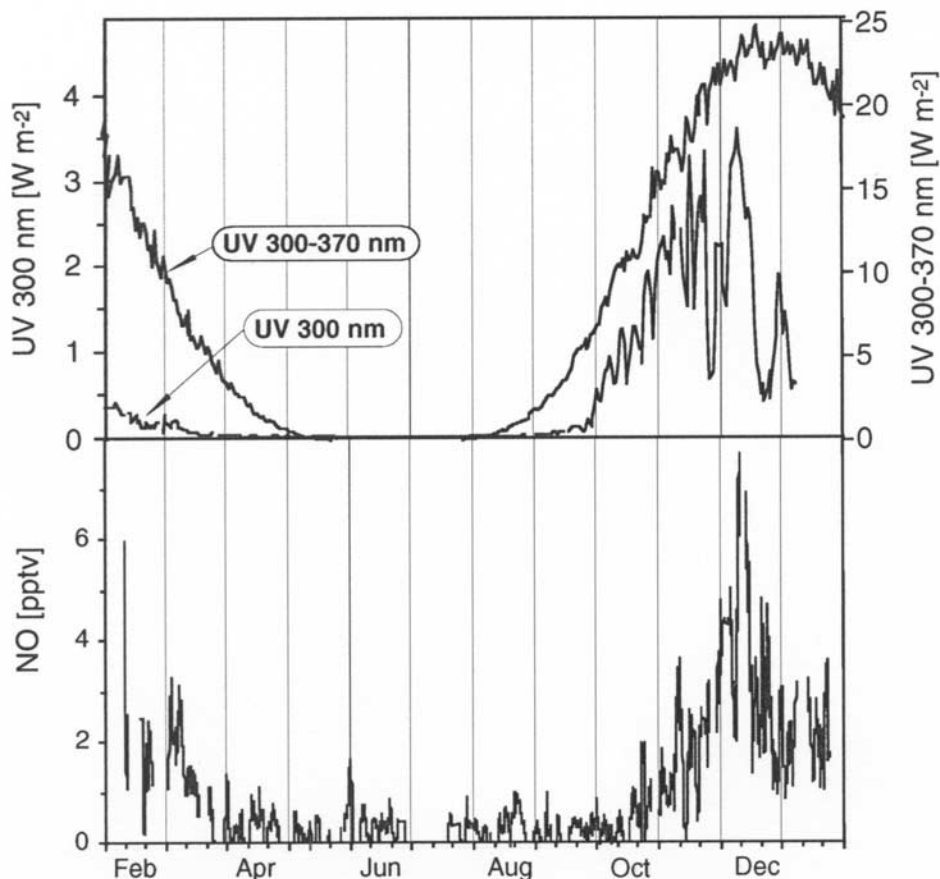


Figure 4. Seasonality of the measured NO mixing ratios (24-hour running means), solar radiation at 300 nm (daily averages, measured by the spectroradiometer), and solar UV radiation from 300 to 370 nm (daily averages, measured by the UV radiometer).

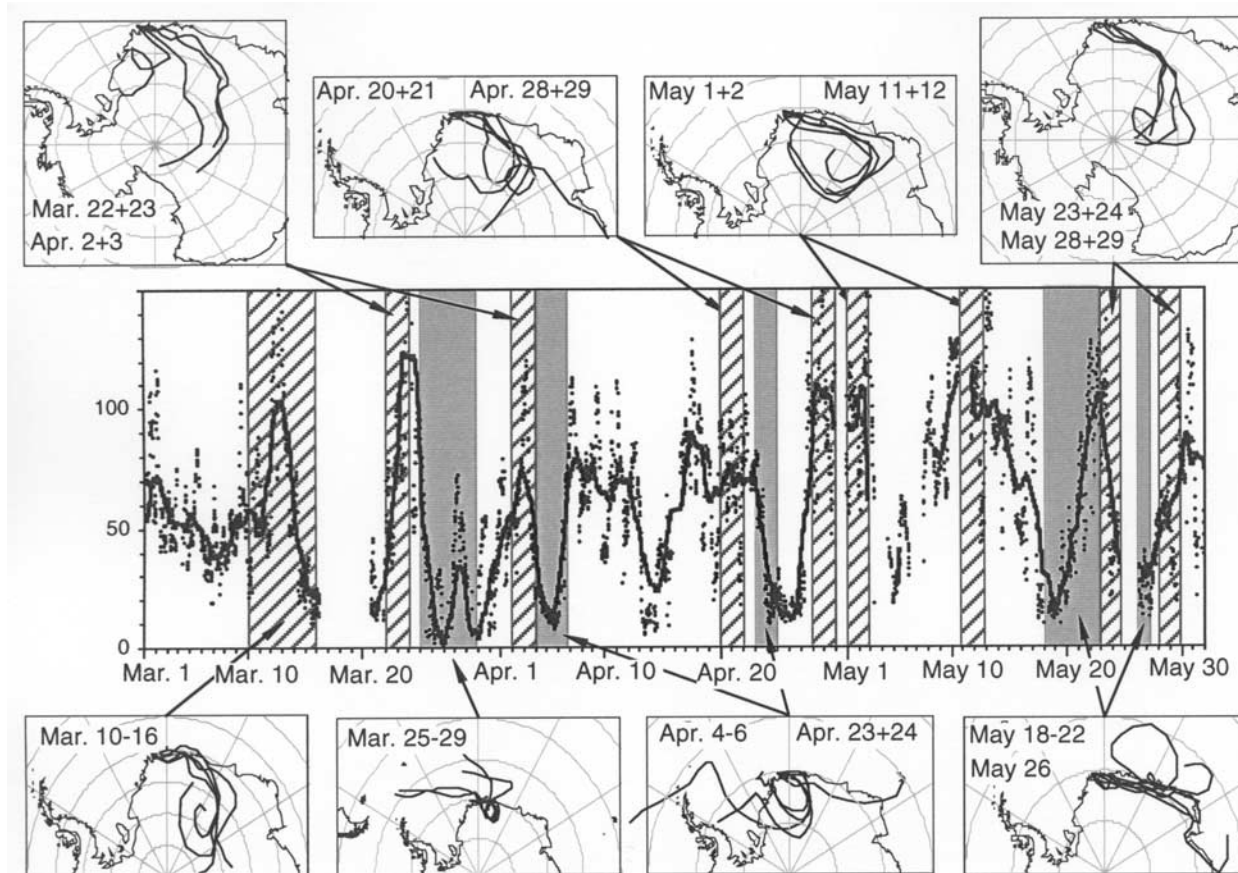


Figure 5. Details of the measured NO_y^* time series from March to May 1999. Dots represent 30-min averages, the gray line corresponds to 24-hour running means. Also shown are 5-day back trajectories arriving at Neumayer at 1200 UTC during marked periods (gray: marine air masses; hatched: air masses from the continental free troposphere.) For details, see text.

tropospheric box inventories are described by the following equation:

$$\frac{[^{10}\text{Be}]}{[^{7}\text{Be}]} = \frac{P_{10} + J_{10}}{P_7 + J_7} \left(1 + \frac{\tau}{\tau_7} \right)$$

P_i and J_i are the production rates and fluxes of the corresponding beryllium isotope ^iBe into the box, τ_7 is the radioactive lifetime of ^7Be (77 days) and τ the residence time of aerosol in the atmospheric box. The production ratio $P_{10}/P_7 = 0.52$ [Masarik and Beer, 1999] is expected to be constant throughout the atmosphere. The stratospheric lifetime used to estimate the stratospheric $^{10}\text{Be}/^7\text{Be}$ ratio is assumed to be 1 year [Raisbeck et al., 1981] which is on the lower end of the range derived from ^{90}Sr profiles by Johnston [1989]. The model is employed to derive the stratospheric ^{10}Be fraction $[^{10}\text{Be}]_{sf}$ seen at Neumayer which in turn is used to estimate the associated stratospherically derived NO_y fraction $[\text{NO}_y]_{sf}$ where $[\text{NO}_y]_s/[^{10}\text{Be}]_s$ denotes the respective ratio in the stratosphere:

$$[\text{NO}_y]_{sf} = [^{10}\text{Be}]_{sf} \left(\frac{[\text{NO}_y]_s}{[^{10}\text{Be}]_s} \right)$$

A stratospheric ^{10}Be concentration of 4×10^6 at scm^{-1} was assumed from respective production rate [Masarik and

Beer, 1999] and aerosol lifetime. The corresponding NO_y mixing ratio in the lower stratosphere varied between 3 and 6 ppbv according to Gao et al. [1997]. Accordingly a range for $([\text{NO}_y]_s/[^{10}\text{Be}]_s)$ between 0.75×10^{-15} and $1.5 \times 10^{-15} \text{ m}^3 \text{ atm}^{-1}$ has been employed. The result of this estimate indicates that the seasonality of surface NO_y at Neumayer could be caused by stratospheric air mass intrusions, although the NO_y^* maximum appeared about 2–3 months later (Figure 8). In addition our admittedly crude estimate demonstrates that most of the NO_y^* measured at Neumayer originated most probably from the stratosphere, leaving little room for a supplementary tropospheric NO_y contribution. Nevertheless a plausible explanation for the observed NO_y^* maximum early May 1999 can not be given on the basis of our results. Note that we used a mean seasonal cycle of the $^{10}\text{Be}/^7\text{Be}$ ratio, because data from 1999 were only available in 3-month means. Accordingly a close coincidence between the seasonality of NO_y^* and $^{10}\text{Be}/^7\text{Be}$ can not be anticipated. The seasonalities of alkyl nitrate and PAN sources coming into question are not clear. However, for these NO_y component species, accounting for about 70% of the total NO_y^* during austral summer at Neumayer, a stratospheric source should be negligible.

[21] Recent field measurements, satellite observations and model simulations suggest lightning activity to play an

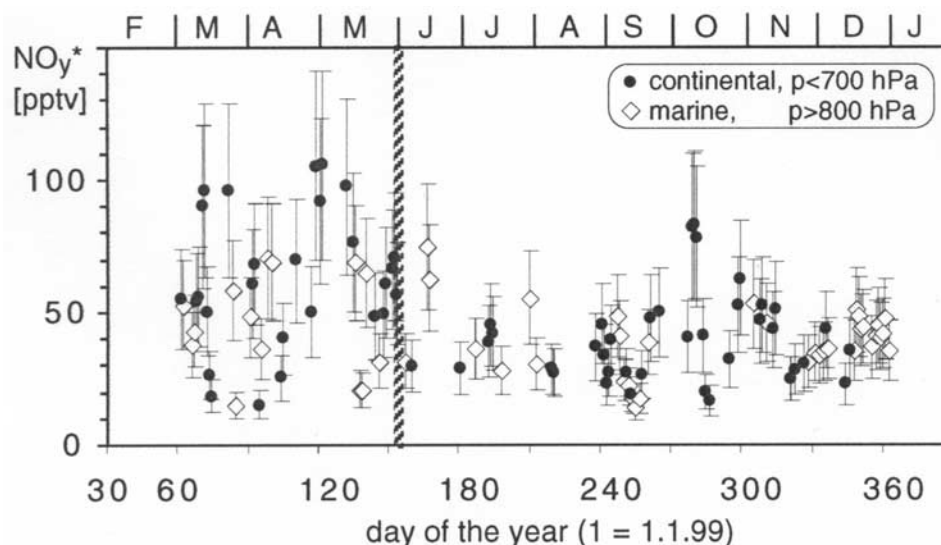


Figure 6. Daily mean NO_y^* mixing ratios classified according to the origin of advected air masses. The line separates the period of high NO_y^* variability. For details, see text.

important role in determining the NO_y budget of the upper troposphere [Zhang *et al.*, 2000; Tie *et al.*, 2001; Bond *et al.*, 2002] and may also be a significant source for Antarctic NO_y . However, the seasonal maximum of lightning activity in southern Africa occurs from December to February [Zhang *et al.*, 2000; Bond *et al.*, 2002], hence preceding the observed NO_y^* maximum at Neumayer by 3–5 months.

3.4. Comparison With Seasonality of Total Nitrate and Arctic NO_y

[22] Our results constitute the first year-round NO_y^* record from Antarctica. From the high Arctic, up to now, the sole seasonal cycle of NO_y^* was recorded by Honrath and Jaffe [1992] at Barrow (a coastal station in Alaska, $71^\circ 19' \text{N}$, $156^\circ 37' \text{W}$) using a similar technique. They

observed maximum NO_y^* mixing ratios of about 500–700 pptv in late winter/early spring while during polar summer median values were as low as 70 pptv. These results are consistent with more recent measurements conducted at Summit, Greenland, during the summers of 1994 and 1995 [Dibb *et al.*, 1998; Munger *et al.*, 1999]. Compared to the Arctic maximum, NO_y^* mixing ratios measured at Neumayer were lower by nearly an order of magnitude with a different seasonal cycle. In the Arctic, maximum total nitrate ($\text{HNO}_3 + \text{p-NO}_3^-$) mixing ratios between 25 and 90 pptv can be found in late January/February [Barrie and Hoff, 1985], while the annual maximum at coastal Antarctic sites is again different and appears in late austral spring (November). In the Arctic, the $\text{HNO}_3/\text{NO}_y^*$ ratio is very low, around 0.01 during summer [Dibb *et al.*, 1998; Munger *et*

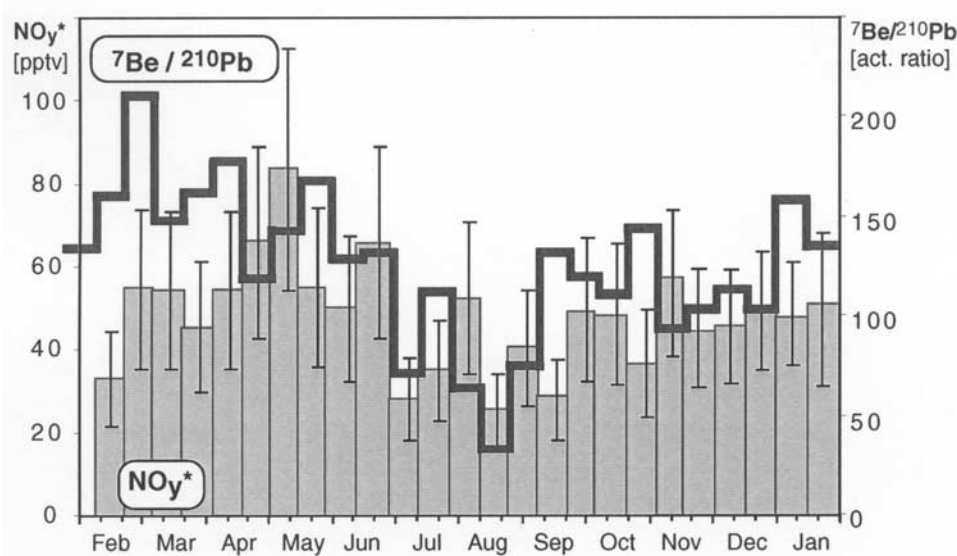


Figure 7. Seasonality of NO_y^* (gray bars) in comparison with ${}^7\text{Be}/{}^{210}\text{Pb}$ activity ratios (thick line). The NO_y^* mixing ratios equal averages for the corresponding radionuclide sampling periods (2 weeks).

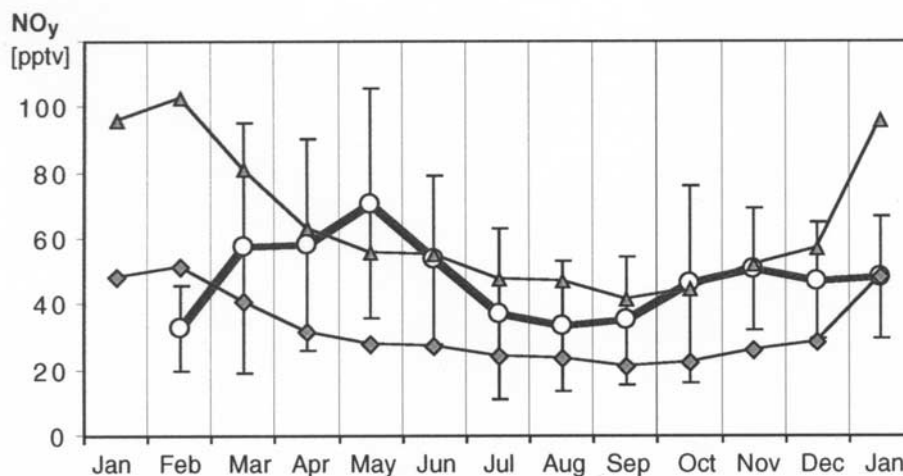


Figure 8. Measured NO_y^* (circles) in comparison with the stratospheric component of NO_y calculated from the ^7Be and ^{10}Be data, assuming a stratospheric NO_y mixing ratio of 3 ppbv (shaded diamonds) and 6 ppbv (shaded triangles). All data have been averaged to calendar months. In addition for NO_y^* , the standard deviation of the individual means is shown.

al., 1999] while at Neumayer a value of 0.31 is typical for the same season. PAN seems to be the dominating reactive nitrogen component in the Arctic, at least during winter and spring [Solberg *et al.*, 1997]. Unfortunately, for Antarctica a NO_y -budget assessment is only possible for February, indicating that organic nitrates, i.e., PAN and methyl nitrate, are the main compounds. A strong impact of industrial emissions, which accumulate in the Arctic troposphere during winter/spring, is evident [Ottar, 1989; Honrath and Jaffé, 1992; Wofsy *et al.*, 1992]. Other important sources for Arctic NO_y are natural fires and intrusions of stratospheric air masses [Wofsy *et al.*, 1992]. In Antarctica, on the other hand, stratospheric input and (sub-) tropical lightning activities were put forward as dominant sources, at best for HNO_3 and p-NO_3^- [Legrand and Delmas, 1986; Wolff, 1995; Wagenbach *et al.*, 1998]. As discussed in detail by Wagenbach *et al.* [1998], the seasonal total nitrate maximum most probably reflects stratospheric nitrate input associated with the sedimentation and evaporation of polar stratospheric clouds (PSCs). The observed seasonal maximum of NO_y^* appeared in April/May, too early for PSC sedimentation but roughly consistent with the annual maximum of stratospheric air mass intrusions. Although the seasonality of the total nitrate and NO_y^* signal at Neumayer is clearly different and thus no obvious correlation between atmospheric nitrate ($\text{HNO}_3 + \text{p-NO}_3^-$) and NO_y^* mixing ratios is evident, the stratosphere seems to be the main source region.

4. Conclusions

[23] Trajectory analyses and radioisotope variability (^7Be , ^{10}Be and ^{210}Pb) consistently indicated an upper tropospheric or stratospheric NO_y^* source region, although the seasonal maximum observed in early May could not be explained by any potential NO_y source. Our results did not support the northward continents or marine boundary layer to be a significant source for NO_y^* measured at Neumayer. Thus our findings support the idea that nitrate signals

archived in Antarctic ice cores under present-day climatic conditions are dominated by a stratospheric source [Wagenbach *et al.*, 1998]. Our results do not indicate a locally enhanced (coastal or ice-edge) marine source of CH_3ONO_2 . Most probably methyl nitrate mixing ratios observed at Neumayer represent a background level induced by uniform marine emissions throughout the Southern Hemisphere. Coinciding year-round measurements of individual NO_y component species, in particular $\text{NO} + \text{NO}_2$, PAN, RONO_2 , and HNO_3 are necessary to overcome ambiguities concerning the source region and budget of Antarctic reactive nitrogen oxides. Present atmospheric models symptomatically overpredict upper tropospheric HNO_3/NO_y ratios indicating a serious shortfall in understanding chemistry and budget of reactive nitrogen oxides in the (global) upper troposphere. Nevertheless, dedicated modeling efforts specifically designed for trace component conversion and transport to Antarctica and for the remobilization of oxidized nitrogen species from the upper firn layer would be indispensable to elucidate possible source regions of NO_y compounds finally controlling ice core nitrate variability.

[24] **Acknowledgments.** The authors would like to thank G. König-Langlo for providing the meteorological data used in this contribution. We also acknowledge the valuable comments of three anonymous referees, which helped to improve the paper. Special thanks go to the technicians and scientists of the Neumayer overwintering crews of the years 1998 and 1999.

References

- Barrie, L. A., and R. M. Hoff, Five years of air chemistry observations in the Canadian Arctic, *Atmos. Environ.*, **19**, 1995–2010, 1985.
- Bodhaine, B. A., Aerosol absorption measurements at Barrow, Mauna Loa, and the South Pole, *J. Geophys. Res.*, **100**, 8967–8975, 1995.
- Bond, D. W., S. Steiger, R. Zhang, X. Tie, and R. Orville, The importance of NO_x production by lightning in the tropics, *Atmos. Environ.*, **36**, 1509–1519, 2002.
- Davis, D., *et al.*, Unexpected high levels of NO observed at the South Pole, *Geophys. Res. Lett.*, **28**, 3625–3628, 2001.
- Dibb, J. E., R. W. Talbot, J. W. Munger, D. J. Jacob, and S.-M. Fan, Air-snow exchange of HNO_3 and NO_y at Summit, Greenland, *J. Geophys. Res.*, **103**, 3475–3486, 1998.

- Fischer, H., D. Wagenbach, and S. Kipfstuhl, Sulfate and nitrate firm concentrations on the Greenland ice sheet, 2, Temporal anthropogenic deposition changes, *J. Geophys. Res.*, *103*, 21,935–21,942, 1998.
- Flocke, F., E. Atlas, S. Madronich, S. M. Schaufli, K. Aikin, J. J. Margitan, and T. P. Bui, Observations of methyl nitrate in the lower stratosphere during STRAT: Implications for its gas phase production mechanisms, *Geophys. Res. Lett.*, *25*, 1891–1894, 1998.
- Gao, R. S., et al., Partitioning of the reactive nitrogen reservoir in the lower stratosphere of the Southern Hemisphere: Observations and modeling, *J. Geophys. Res.*, *102*, 3935–3949, 1997.
- Honrath, R. E., and D. A. Jaffe, The seasonal cycle of nitrogen oxides in the arctic troposphere at Barrow, Alaska, *J. Geophys. Res.*, *97*, 20,615–20,630, 1992.
- Honrath, R. E., M. C. Peterson, S. Guo, J. E. Dibb, P. B. Shelson, and B. Cambell, Evidence of NO_x production within or upon ice particles in the Greenland snowpack, *Geophys. Res. Lett.*, *26*, 695–698, 1999.
- Jacobi, H.-W., R. Weller, T. Bluszcz, and O. Schrems, Latitudinal distribution of peroxyacetyl nitrate (PAN) over the Atlantic Ocean, *J. Geophys. Res.*, *104*, 26,901–26,912, 1999.
- Jacobi, H.-W., R. Weller, A. E. Jones, P. S. Anderson, and O. Schrems, Peroxyacetyl nitrate (PAN) concentrations in the Antarctic troposphere measured during the photochemical experiment at Neumayer (PEAN'99), *Atmos. Environ.*, *34*, 5235–5247, 2000.
- Jones, A. E., R. Weller, A. Minikin, E. W. Wolff, W. T. Sturges, H. P. McIntyre, S. R. Leonard, O. Schrems, and S. Bauguitte, Oxidized nitrogen chemistry and speciation in the Antarctic troposphere, *J. Geophys. Res.*, *104*, 21,355–21,366, 1999.
- Jones, A. E., R. Weller, E. W. Wolff, and H.-W. Jacobi, Speciation and rate of photochemical NO and NO₂ production in Antarctic snow, *Geophys. Res. Lett.*, *27*, 345–348, 2000.
- Jones, A. E., R. Weller, P. S. Anderson, H.-W. Jacobi, E. W. Wolff, O. Schrems, and H. Miller, Measurements of NO_x emissions from the Antarctic snowpack, *Geophys. Res. Lett.*, *28*, 1499–1502, 2001.
- Johnston, H., Evaluation of excess carbon 14 and strontium 90 data for suitability to test two-dimensional stratospheric models, *J. Geophys. Res.*, *94*, 18,485–18,493, 1989.
- Junkermann, W., U. Platt, and A. Volz-Thomas, A photoelectric detector for the measurement of photolysis frequencies of ozone and other atmospheric molecules, *J. Atmos. Chem.*, *8*, 203–227, 1989.
- Kleinman, L. I., Low and high NO_x tropospheric photochemistry, *J. Geophys. Res.*, *99*, 16,831–16,838, 1994.
- König-Langlo, G., J. C. King, and P. Pettré, Climatology of the three coastal Antarctic stations Dumont d'Urville, Neumayer, and Halley, *J. Geophys. Res.*, *103*, 10,935–10,946, 1998.
- Kottmeier, C., and B. Fay, Trajectories in the Antarctic lower troposphere, *J. Geophys. Res.*, *103*, 10,947–10,959, 1998.
- Legrand, M. R., and R. J. Delmas, Relative contributions of tropospheric and stratospheric sources to nitrate in Antarctic snow, *Tellus*, *38B*, 236–249, 1986.
- Legrand, M., and P. Mayewski, Glaciochemistry of polar ice cores: A review, *Rev. Geophys.*, *35*, 219–243, 1997.
- Logan, J. A., M. J. Prather, S. C. Wofsy, and M. B. McElroy, Tropospheric chemistry: A global perspective, *J. Geophys. Res.*, *86*, 7210–7254, 1981.
- Logan, J. A., Nitrogen oxides in the troposphere: Global and regional budgets, *J. Geophys. Res.*, *88*, 10,785–10,807, 1983.
- McIntyre, H. P., The measurement and implications of short chain alkyl mono-nitrates in contemporary tropospheric and aged polar firm air, Ph.D. thesis, Univ. of East Anglia, Norwich, UK, 2001.
- Masarik, J., and J. Beer, Simulation of particle fluxes and cosmogenic nuclide production in the Earth's atmosphere, *J. Geophys. Res.*, *104*, 12,099–12,111, 1999.
- Munger, J. W., D. J. Jacob, S.-M. Fan, A. S. Colman, and J. E. Dibb, Concentration and snow-atmosphere fluxes of reactive nitrogen at Summit, Greenland, *J. Geophys. Res.*, *104*, 13,721–13,734, 1999.
- Ottar, B., Arctic air pollution: A Norwegian perspective, *Atmos. Environ.*, *23*, 2349–2356, 1989.
- Raisbeck, G. M., F. Yiou, M. Fruneau, J. M. Loiseaux, M. Lieveu, and J. C. Ravel, Cosmogenic ¹⁰Be/⁷Be as a probe of atmospheric transport processes, *Geophys. Res. Lett.*, *8*, 1015–1018, 1981.
- Röthlisberger, R., et al., Nitrate in Greenland and Antarctic ice cores: A detailed description of post-depositional processes, *Ann. Glaciol.*, in press, 2002.
- Schoeberl, M. R., and D. L. Hartmann, The dynamics of the stratospheric polar vortex and its relation to springtime ozone depletions, *Science*, *251*, 46–52, 1991.
- Schrumpf, W., K. P. Müller, F. J. Johnen, K. Lienaerts, and J. Rudolph, An optimized method for airborne peroxyacetyl nitrate (PAN) measurements, *J. Atmos. Chem.*, *22*, 303–317, 1995.
- Seckmeyer, G., B. Mayer, and G. Bernhard, The 1997 status of solar UV spectroradiometry in Germany: Results from the national intercomparison of UV spectroradiometers Garmisch Partenkirchen, Germany, in *Fraunhofer Institut Atmosphärische Umweltforschung Schriftenreihe*, vol. 55, edited by W. Seiler, pp. 1–166, Shaker Verlag, Aachen, 1998.
- Shaw, G. E., On the resident time of Antarctic ice sheet sulfate aerosol, *J. Geophys. Res.*, *87*, 4309–4313, 1982.
- Solberg, S., T. Krognnes, F. Stordal, Ø. Hov, H. J. Beine, D. A. Jaffe, K. C. Clemitshaw, and S. A. Penkett, Reactive nitrogen compounds at Spitsbergen in the Norwegian Arctic, *J. Atmos. Chem.*, *28*, 209–225, 1997.
- Talbot, R. W., et al., Tropospheric reactive odd nitrogen over the South Pacific in austral springtime, *J. Geophys. Res.*, *105*, 6681–6694, 2000.
- Thakur, A. N., H. B. Singh, P. Mariani, Y. Chen, Y. Wang, D. J. Jacob, G. Brasseur, J.-F. Müller, and M. Lawrence, Distribution of reactive nitrogen species in the remote free troposphere: Data and model comparisons, *Atmos. Environ.*, *33*, 1403–1422, 1999.
- Tie, X., R. Zhang, G. Brasseur, L. Emmons, and W. Lei, Effects of lightning on reactive nitrogen and nitrogen reservoir species in the troposphere, *J. Geophys. Res.*, *106*, 3167–3178, 2001.
- Wagenbach, D., U. Görlach, K. Moser, and K. O. Münnich, Coastal Antarctic aerosol: The seasonal pattern of its chemical composition and radionuclide content, *Tellus*, *40B*, 426–436, 1988.
- Wagenbach, D., Coastal Antarctica: Atmospheric chemical composition and atmospheric transport, in *Chemical Exchange Between the Atmosphere and Polar Snow*, NATO ASI Ser., vol. 43, edited by E. W. Wolff and R. C. Bales, pp. 173–199, Springer-Verlag, New York, 1996.
- Wagenbach, D., M. Legrand, H. Fischer, F. Pichlmayer, and E. W. Wolff, Atmospheric near-surface nitrate at coastal Antarctic sites, *J. Geophys. Res.*, *103*, 11,007–11,020, 1998.
- Weller, R., and O. Schrems, Photooxidants in the marine Arctic troposphere in summer, *J. Geophys. Res.*, *101*, 9139–9147, 1996.
- Weller, R., A. Minikin, G. König-Langlo, O. Schrems, A. E. Jones, E. W. Wolff, and P. S. Anderson, Investigating possible causes of the observed diurnal variability in Antarctic NO_y, *Geophys. Res. Lett.*, *26*, 2853–2856, 1999.
- Wofsy, S. C., et al., Atmospheric chemistry in the Arctic and Subarctic: Influence of natural fires, industrial emissions, and stratospheric inputs, *J. Geophys. Res.*, *97*, 16,731–16,746, 1992.
- Wolff, E. W., Nitrate in polar ice, in *Ice Core Studies of Global Biogeochemical Cycles*, NATO ASI Ser., vol. 30, edited by R. J. Delmas, pp. 195–224, Springer-Verlag, New York, 1995.
- Wolff, E. W., and H. Cachier, Concentrations and seasonal cycle of black carbon in aerosol at a coastal Antarctic station, *J. Geophys. Res.*, *103*, 11,033–11,041, 1998.
- Zellweger, C., M. Ammann, B. Buchmann, P. Hofer, M. Lugauer, R. Rüttimann, N. Streit, E. Weingartner, and U. Baltensperger, Summertime NO_y speciation at the Jungfrauoch, 3580 m above sea level, Switzerland, *J. Geophys. Res.*, *105*, 6655–6667, 2000.
- Zhang, R., N. T. Sanger, R. E. Orville, X. Tie, W. Randel, and E. R. Williams, Enhanced NO_x by lightning in the upper troposphere and lower stratosphere inferred from the UARS global NO₂ measurements, *Geophys. Res. Lett.*, *27*, 685–688, 2000.

M. Huke and D. Wagenbach, Institut für Umwelphysik, Universität Heidelberg, D-69120 Heidelberg, Germany.

H.-W. Jacobi and R. Weller, Alfred-Wegener-Institut für Polar- und Meeresforschung, D-27570 Bremerhaven, Germany. (rweller@awi-bremerhaven.de)

A. E. Jones, British Antarctic Survey, Natural Environment Research Council, High Cross, Madingley Road, Cambridge CB3 0ET, UK.

H. P. McIntyre and W. T. Sturges, School of Environmental Sciences, University of East Anglia, Norwich NR4 7TJ, UK.

A. Wille, Metrohm AG, CH-9101 Herisau, Switzerland.